Preprint Title Hydrothermal synthesis of carbon nanodots from wine cork and biocompatible fluorescent probe

Authors Ngo Khoa Quang, Nguyen Ngoc Hieu, Vo Van Quoc Bao, Vo Thi Phuoc, Le Xuan Diem Ngoc, Luong Quang Doc, Nguyen Minh Tri, Le Vu Truong Son, Le Van Thanh Son and Che Thi Cam Ha

Publication Date 09 Juni 2021

Article Type Full Research Paper

ORCID® iDs Ngo Khoa Quang - https://orcid.org/0000-0003-3241-178X; Nguyen Ngoc Hieu - https://orcid.org/0000-0001-6091-3491; Le Vu Truong Son - https://orcid.org/0000-0002-1724-0137; Le Van Thanh Son - https://orcid.org/0000-0002-2061-6983

Hydrothermal synthesis of carbon nanodots from wine cork and biocompatible fluorescent probe

Ngo Khoa Quang*[1], Nguyen Ngoc Hieu[2,3], Vo Van Quoc Bao[4], Vo Thi Phuoc[1], Le Xuan Diem Ngoc[1], Luong Quang Doc[1],Nguyen Minh Tri[1], Le Vu Truong Son[5], Le Van Thanh Son[5] and Che Thi Cam Ha[1]

Address: [1]University of Sciences, Hue University, 77 Nguyen Hue, Hue, Vietnam, [2]Faculty of Environmalet and Chemical Engineering, Duy Tan University, Da Nang, 550000, Vietnam, [3]Institute for Research and Training in Medince, Biology and Pharmacy, Duy Tan University, Da Nang, 550000, Vietnam, [4]University of Agriculture and Forestry, Hue University, 102 Phung Hung, Hue, Vietnam, [5]Faculty of Physics, University of Science and Education, The University of Da Nang, 459 Ton Duc Thang, Lien Chieu, Da Nang, Vietnam

Email: Ngo Khoa Quang - nkquang@hueuni.edu.vn

* Corresponding author

Abstract

We presented a low-cost and simple method to synthesize carbon nanodots (CDs) from waste wine cork using hydrothermal synthesis. The structural and optical properties of the CDs are characterized by TEM, FTIR, Raman, UV-Vis absorption, and photoluminescence (PL) spectra. The analysis results indicated the average diameter of CDs ~ 6.2 ± 2.7 nm. Optical measurements showed the phenomenon of excitation-dependent PL and the formation of functional groups on the surface of the

particles. CDs with a quantum yield of 1.54% was calculated using quinine sulfate as reference. Furthermore, a probe of wine cork-derived CDs in bioimaging has been successfully applied in living mesenchymal stem cells (MSCs). After treatment with CDs, MSCs exhibited fluorescence including green, yellow, and red colors under the excitation wavelengths in the range 330–385 nm, 450–480 nm, and 510–550 nm, respectively. The achievement demonstrated potential applications of fluorescent CDs in the field of the fluorescent image.

Keywords

carbon nanodots; hydrothermal synthesis; fluorescence; fluorescent image; waste wine cork

Introduction

Recent nanostructure fabrication methods have allowed researchers to synthesize materials with revolutionary potential applications [1-4]. There are multiple ways to prepare substances at the nanoscale based on the proposal whereby it can be divided into two routes, bottom-up and top-down [5-12]. The development of fabrication techniques offers many advantages. At the same time, it also prompts scientists to search for novel nanoscale materials, overcoming the limitations of conventional ones. In terms of carbon nanomaterials, the discovery of carbon nanodots (CDs) should be a case. Although CDs were accidentally discovered by Xu et al when they purified single-walled carbon nanotubes, CDs constitute an active area of fluorescent materials, driven by fundamental questions related to many intriguing optical features [13].

CDs have been defined as carbon nanoparticles with sizes below 10 nm [14,15]. CDs are specifically novel kinds of nanoparticles possessing intrinsically optical properties, which have been associated with high biocompatibility, excellent photostability, as well as the phenomenon of excitation-dependent photoluminescence [16-21]. Hence, in recent years, numerous research groups have reported a broad range of applications of CDs including biological labeling, drug delivery, chemical and biosensors, bioimaging, electrocatalysis, etc [22-25]. For biomedical applications, CDs are considered as a potential solution of future expectation of fluorescent nanomaterials since it takes advantage of traditional semiconductor quantum dots together with their unique characteristic of likely lower cytotoxicity [20, 26, 27].

For synthesizing CDs, a green and simple preparation is highly desired to overcome the limitation of complex synthesis routes, the involvement of toxic, or expensive reagents. In recent years, the hydrothermal method is considered a cost-effective chemical route for the conversion of carbonization [28-32]. The technique can achieve carbonaceous materials from widely available precursors. Not only the chemical reagents but also the natural sources are favorable to this treatment. Previous works have addressed green biomass precursors could provide an ideal strategy to prepare green fluorescent CDs, especially the waste materials [33-37].

Herein is described the preparation of CDs from waste wine cork (made by cork oak) by hydrothermal treatment. The rationale for the selection of wine cork is considered concerning the polysaccharides content of cork up to 20.9% in the chemical composition [38]. As previously published, many preparations of the polysaccharides-rich material were successfully employed to synthesize CDs [39]. To access the characterization of the obtained CDs, we investigated using analytical techniques, including TEM, FTIR, UV-Vis absorption, and photoluminescence (PL) spectra. Furthermore, we attempted to probe biocompatibility by incubating mesenchymal stem

cells (MSCs) from human umbilical cord (UC) with the obtained CDs. It would provide us information in an adjustment of the CDs synthesized from waste wine cork for bioimaging applications.

Results and Discussion

From the photo presented in Figure 1a, we can see that the aqueous solution containing obtained CDs shows the visible green color under laser irradiation of 405 nm wavelength. In comparison to that under room light, this evidence confirms the formation of fluorescent production to be seen with the naked eyes. As can be seen from Figure 1b, the TEM indeed indicated the obtained particles have a uniform dispersion without obvious aggregation. Specifically, the size histogram of particles presented in Figure 1c indicated the average diameter of CDs ~ 6.2 ± 2.7 nm and the value was comparable to the previous report [35,36].

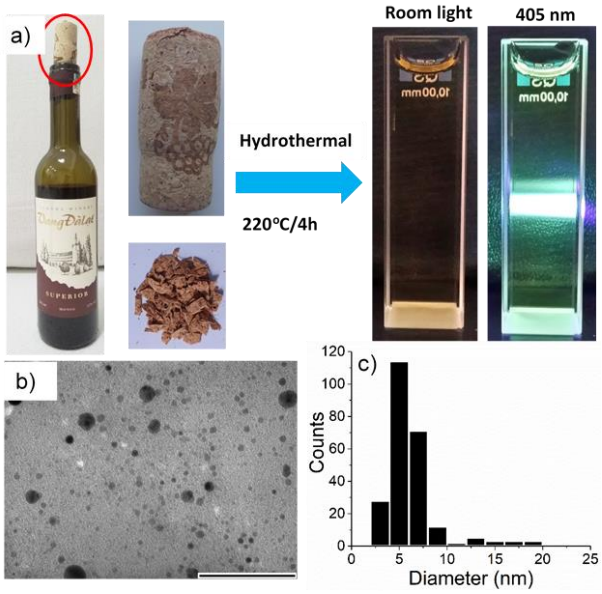

Figure 1: (a) Illustration of the CDs synthesis process of wine cork and photos of CDs solution under room light and 405 nm laser light. (b) TEM image of the obtained CDs with the scale bar is 100 nm and (c) the corresponding size distribution.

The phase of the obtained CDs was clarified by X-ray diffraction (XRD) pattern and Raman spectra. The XRD shown in Figure 2a illustrated a broad peak at 2θ~22^{o} and this should be consistent with the (002) lattice spacing, a formation of highly amorphous carbon-based materials [18]. Moreover, the Raman spectra show an intense peak and a shoulder at around 1370 and 1570 cm^{-1}, which confirmed the existence of both D (sp^3 hybridized carbon atoms) and G (vibrations of sp^2 hybridized carbon atoms) bands [40]. The result obtained in Figure 2b further proves the amorphous nature of the wine cork-derived CDs [40,41].

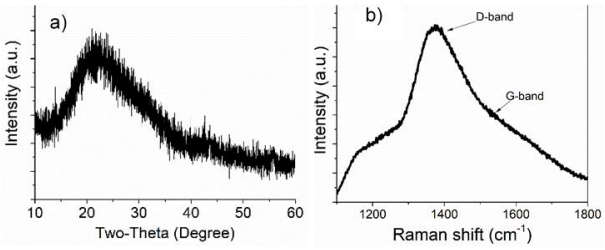

Figure 2: (a) The XRD pattern and (b) Raman spectrum of the obtained CDs.

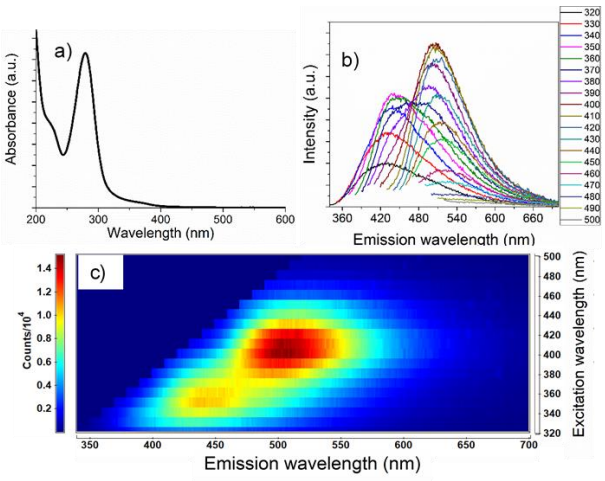

Figure 3: (a) UV–Vis absorption spectra of CDs. (b) The PL spectra of obtained CDs under different excitation wavelengths from 320 to 500 nm (in 10 nm increments starting from 320 nm) and (c) corresponding contour plot.

The optical properties of CDs were investigated by UV-vis absorption and emission spectra. CDs with a quantum yield of 1.54% was calculated using quinine sulfate as

reference. The UV-vis absorption spectrum shown in Figure 3a indicates two peaks around 217 and 280 nm. Similar UV–vis spectrum were reported in previous publications, these are attributed to $\pi-\pi^*$ transition of the C=C and $n-\pi^*$ transition of the C=O bonds, respectively [40]. To further clarify optical behavior, we examined fluorescence spectra of the obtained CDs. In early studies, CDs exhibits the dependence of the emission on the excitation wavelength [36,40]. Similarly, in our case, there is an obvious shift as the excitation wavelength varies, as shown in Figure 3b. Particularly, the corresponding contour shown in Figure 3c revealed two fluorescence bands with the emission intensity achieved the strongest value in the longer excitation wavelength region. In a previous publication, Pyng Yu et al. showed evidence of dual fluorescence bands when they investigated the temperature-dependent spectroscopic results of CDs [42]. The shorter emission band was attributed to the core state emission, whereas the longer one resulted from the surface state emission. More recently, it has been found that fluorescent CDs synthesized from tofu wastewater also presented this effect, in which high and low energy bands have peaks at about 450 and 490 nm, respectively [43]. Up to now, the physical mechanism for photon-induced light emission from CDs is still unclear. The difficult issue is to estimate the role of carbon core and functional groups to the PL spectra and examination of these effects is still a significant challenge. Researchers have proposed that the possible candidate for the physical origin could be attributed to the optical selection of surface state owing to hybridization of the carbon core and the functional groups [20,44,45].

Subsequently, the chemical structure and composition of functional groups onto the surfaces of the CDs during the thermal reaction were investigated using a FITR spectrum. The result is shown in Figure 4. The characteristic absorption bands indeed reflect the functional groups, including an O–H stretching vibration at 3421 cm^{-1}, C-H

stretching vibration at 2927 and 2856 cm^{-1}, N–H bending vibration at 1651 cm^{-1}, C=O stretching vibration at 1631 cm^{-1} [36,46-48]. In addition, peaks at 1402 and 1060 cm^{-1} result from the C–O–C asymmetric and symmetric vibrational stretch [49]. According to the above-mentioned assignments, the FTIR spectrum revealed the functional groups on the surface of the carbon core after the thermal reaction. Since these play a very important role in bioconjugation, this promoted us in further probe bioimaging of the obtained CDs.

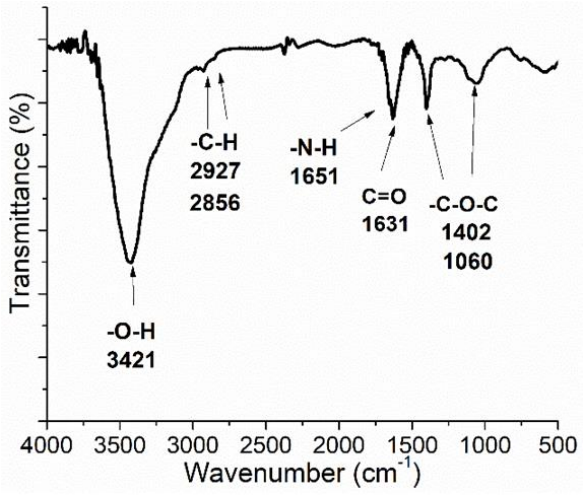

Figure 4: FTIR spectrum reflects the functional groups were introduced onto the surface of CDs.

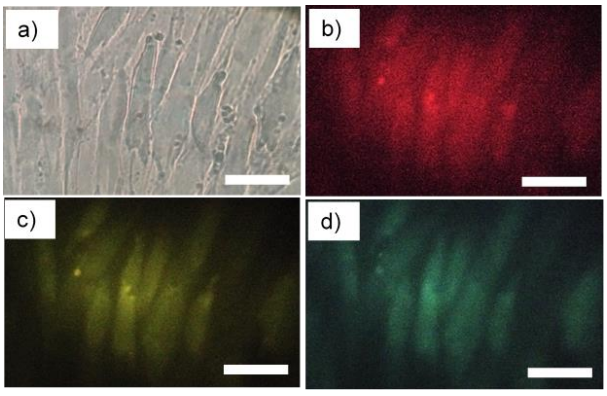

Figure 5: Optical microscopy of mesenchymal stem cells. MSCs incubated with the obtained CDs (a) under transmission light and (b) green (515–560 nm), (c) blue (450–490 nm), and (d) violet (320–380 nm) light excitation. Scale bar is 50 µm.

Namely, fluorescent images of the MSCs incubated with the obtained CDs are shown in Figure 5. In the bright-field optical image, the cells showed no substantial change in shape after the wine cork-derived CDs treatment. As shown in Figure 5b, 5c and 5d, MSCs exhibited fluorescence including green, yellow, and red colors under violet (320–380 nm), blue (450–490 nm), and green (515–560 nm) light excitation, respectively. Meanwhile, the control sample with no treatment of the CDs showed no photoluminescence at the same exposure conditions (data not shown). The results are consistent with the previous publications [19,50,51]. The excitation-dependent PL made it possible for multiple color emission in cells imaged by using CDs only. A possible mechanism of CDs uptake by MSCs is not fully understood and still needs future effort to explain. Up to now, the possible origin could result from the endocytosis mechanism [26,34].

Conclusion

In this study, we successfully synthesized multi colorful fluorescent carbon dots from waste natural precursors using hydrothermal synthesis. The wine cork-derived CDs exhibited bright fluorescence under different excitation wavelengths. Furthermore, the first probe of wine cork-derived CDs has been successfully applied in living MSCs imaging. The result showed that the obtained CDs could be employed as a solution for bioimaging owing to their bright and multicolor luminescence. The achievements suggest further consideration in both the field of photoluminescence and fluorescent image applications.

Experimental

Materials

DMEM/F12 medium, fetal bovine serum (FBS), and proxacin were purchased from Miltenyi Biotec, Germany.

Synthesis of CDs

The waste wine cork (5.0 g) was first washed with water to remove surface dirt and dried in an oven before cutting into small pieces. Then, these were mixed with 80 mL of distilled water to transfer into a 100 mL Teflon-lined autoclave. The resulting mixture was then heated at 220^{o}C for a period of 4 h in an oven. After cooling down to room temperature naturally, the brown-black carbonized solution was roughly purified through a 0.22 µm microporous membrane. Subsequently, the solution was centrifuged at 14000 rpm for 15 min to remove the large particles. Finally, the obtained CDs were stored at 4^{o}C for further use.

In vitro cell imaging with CDs

The commercial mesenchymal stem cells (MSCs) of the human umbilical cord (UC) were purchased with the support of Hue Central Hospital of Obstetrics and Gynecology Department and under the permission of Hematology- Transfusion National Center of Hue Central Hospital (Hue, Vietnam). Then, the MSCs (1×10^3 cells/cm^2) were cultured on a 6-well plate, in the growth medium DMEM/F12 supplemented with 10% FBS and 1% proxacin. The cells were incubated in a humidified atmosphere containing 5 % CO_2 and 95 % air at 37 °C, continuously for 5 - 6 weeks. Twice a week, the medium was substituted, and morphology was examined under the inverted optical microscope. When the cells were approximately 60% confluent, the CDs solution with a

concentration of 0.25× (1× = 0.51 mg/mL) was deliberately added to the cell dishes. The reason for the word ‘deliberately’ is that the cell viability at the concentrations of 0.5×, 0.75× and 1× dramatically decreased upon increasing of exposure time, indicating their less efficiency for the growth of the cells. Details of the cytotoxic effect and related discussions are currently included in an article under preparation (manuscript in preparation). After a further 2 hours incubation, the cells were washed with PBS three times to remove the free CDs attached on the outer surface of the cell membrane. Cell fluorescent images were detected with the excitation wavelengths were set in a range 330–385 nm, 450–480 nm, and 510–550 nm, respectively.

Quantum yield (QY) measurements

CDs with a quantum yield of 1.54% was calculated using quinine sulfate as reference. The quantum yield of the CDs was determined by a comparative method in which Quinine sulfate (literature QY = 0.54) was used as a reference. Four concentrations of each compound were made and the CDs sample was dissolved in water (refractive index (n) of 1.33) while Quinine sulfate dissolved in 0.1 M H_2SO_4 (n = 1.33). All the absorbance values of the solutions at the excitation wavelength were less than 0.1. Photoluminescence (PL) emission spectra of all the sample solutions were recorded at an excitation wavelength of 340 nm. The integrated fluorescence intensity is the area under the PL curve in the wavelength range from 360 to 700 nm. The QY is calculated using the slope of the line determined from the plot of the absorbance against the integrated fluorescence intensities as in equation $QY = QY_r.(m/m_r).(n^2/n^2_r)$. Where m is the slope, n is the refractive index of solvent, and the subscript “r” refers to the referenced sample.

Instrument

We investigated the structural characterization of the obtained CDs by carrying out X-Ray diffraction (XRD) on a D8 Advance (Bruker, Germany) in the range from 10^o to 60^o. To observe the size and morphology of the CDs, we used a transmission electron microscopy (TEM) JEOL JEM–1010 (JEOL, Japan) with an accelerating voltage of 80 kV. For optical properties, UV–vis absorption spectra of the samples were recorded on a GENESYS 10S UV-Vis (Thermo Scientific, American). Fluorescence spectroscopy was carried out on a FS5 spectrofluorometer (Edinburgh Instrument, UK). Fourier-transform infrared (FTIR) spectroscopy on FTIR Affinity-1S (Shimadzu, Japan). The Raman spectrum of obtained samples was recorded with Horiba XploRA PLUS (Horiba, Japan), using excitation at 785 nm. Fluorescence imaging studies were performed with an optical microscope Leica DM2500 (Leica, Germany) and the specimens were excited by a halogen lamp in a range 330–385 nm, 450–480 nm, and 510–550 nm, respectively.

Acknowledgements

We gratefully acknowledge the financial support of the Vietnam Ministry of Education and Training, Grant No. B2021-DHH-05.

References

1. Li, H.; Kang, Z.; Liu, Y.; Lee, S.-T. *J. Mater. Chem.* **2012,** *22*, 24230-24253. doi:10.1039/c2jm34690g

2. Wang, Y.; Hu, A. *J. Mater. Chem. C.* **2014**, *2*, 6921-6939. doi:10.1039/c4tc00988f

3. Liu, M. L.; Chen, B. B.; Li, C. M.; Huang, C. Z. *Green Chem.* **2019**, *21*, 449-471. doi:10.1039/c8gc02736f

4. Meng, W.; Bai, X.; Wang, B.; Liu, Z.; Lu, S.; Yang, B. *Energy Environ. Mater.* **2019**, *2*, 172-192. doi:10.1002/eem2.12038.

5. Sun, Y.-P.; Zhou, B.; Lin, Y.; Wang W.; Fernando, K. A. S.; Pathak, P.; Meziani, M. J.; Harruff, B. A.; Wang, X.; Wang, H.; Luo, P. G.; Yang, H.; Kose, M. E.; Chen, B**.;** Veca, L. M.; Xie, S.-Y. *J. Am. Chem. Soc.* **2006**, *128*, 7756-7757. doi:10.1021/ja062677d

6. Hu, S.-L.; Niu, K.-Y.; Sun, J.; Yang, J.; Zhao, N.-Q.; Du, X.-W. *J. Mater. Chem*. **2009**, *19*, 484-488. doi:10.1039/b812943f

7. Zhou, J.; Booker, C.; Li, R.; Zhou, X.; Sham, T.-K.; Sun, X.; Ding, Z. *J. Am. Chem. Soc*. **2007**, *129*, 744-745. doi:10.1021/ja0669070

8. Liu, H.; Ye, T.; Mao, C. *Angew. Chem. Int. Ed*. **2007**, *46*, 6473-6475. doi:10.1002/anie.200701271

9. Zhu, H.; Wang, X.; Li, Y.; Wang, Z.; Yang, F.; Yang, X. *Chem. Commun*. **2009**, *34*, 5118-5120. doi:10.1039/b907612c

10. Qu, S.; Wang, X.; Lu, Q.; Liu, X.; Wang, L. *Angew. Chem. Int. Ed*. **2012**, *51*, 12215-12218. doi:10.1002/anie.201206791

11. Liu, R.; Wu, D.; Liu, S.; Koynov, K.; Knoll, W.; Li, Q. *Angew. Chem. Int. Ed*. **2009**, *121*, 4668-4671. doi:10.1002/anie.200900652

12. Sun, X.; Brückner, C.; Lei, Y. *Nanoscale*. **2015**, *7*, 17278-17282. doi:10.1039/c5nr05549k

13. Xu, X.-Y.; Ray, R.; Gu, Y.-L.; Ploehn, H. J.; Gearheart, L.; Raker, K.; Scrivens, W. A. *J. Am. Chem. Soc.* **2004**, *126*, 12736-12737. doi:10.1021/ja040082h

14. Nevar, A.; Tarasenka, N.; Nedelko, M.; Tarasenko, N. *Carbon Lett.* **2021**, *31*, 39-46. doi:10.1007/s42823-020-00147-9

15. Yang, N.; Jiang, X.; Pang, D. W. *Carbon Nanoparticles and Nanostructures*; Springer, Switzerland, **2016**, pp. 243-249.

16. Zhou, J.; Sheng, Z.; Han, H.; Zou, M.; Li, C. *Mater. Lett*. **2012**, *66*, 222-224. doi:10.1016/j.matlet.2011.08.081

17. Lim, S.Y.; Shen, W.; Gao, Z. *Chem. Soc. Rev.* **2015**, *44*, 362-381. doi:10.1039/c4cs00269e

18. Sahu, S.; Behera, B.; Maiti, T. K.; Mohapatra, S. *Chem. Commun*. **2012**, *48*, 8835-8837. doi:10.1039/c2cc33796g

19. Shen, P.; Gao, J.; Cong, J.; Liu, Z.; Li, C.; Yao, J. *ChemistrySelect*. **2016**, *1*, 1314-1317. doi:10.1002/slct.201600216

20. Quang, N. K.; Ha, C. T. C. *MRS Advances*. **2019**, *4*, 249-254. doi:10.1557/adv.2019.12

21. Cao, L.; Wang, X.; Meziani, M.J.; Lu, F.; Wang, H.; Luo, P. G.; Lin, Y.; Harruff, B. A.; Vace, L. M.; Murray, D. *J. Am. Chem. Soc.* **2007**, *129*, 11318-11319. doi:10.1021/ja073527l

22. He, L., Wang, T.; An, J.; Li, X.; Zhang, L.; Li, L.; Li, G.; Wu, X.; Su, Z.; Wang, C. *CrystEngComm*. **2014**, *16*, 3259-3263. doi:10.1039/c3ce42506a

23. Liang, Y.; Zhang, H.; Zhang, Y.; Chen, F. *Anal. Methods***. 2015, *7***, 7540-7547. doi:10.1039/c5ay01301a

24. Li, H.; Zhang, Y.; Wang, L.; Tian, J.; Zun, X. *Chem. Commun.* **2011, *47*,** 961-963. doi:10.1039/c0cc04326e

25. Li, H.; Chen, L.; Wu, H.; He, H.; Jin, Y. *Langmuir.* **2014**, *30*, 15016-15021. doi:10.1021/la503729v

26. Baker, S. N.; Baker, G. A. *Angew. Chem. Int. Ed.* **2010**, *38*, 6726-6744. doi:10.1002/anie.200906623

27. Yang, Y.; Cui, J.; Zheng, M.; Hu, C.; Tan, S.; Xiao, Y.; Yanga, Q.; Liu, Y. *Chem. Commun*. **2012**, ***48***, 380-382. doi.org/10.1039/C1CC15678K

28. Dong, Y.; Pang, H.; Yang, H. B.; Guo, C.; Shao, J.; Chi, Y.; Li, C. M.; Yu, T. *Angew. Chem. Int. Ed.* **2013**, *52*, 7800-7804. doi:10.1002/anie.201301114

29. Jin, X.; Sun, X.; Chen, G.; Ding, L.; Li, Y.; Liu, Z.; Wang, Z.; Pan, W.; Hu, C.; Wang, J. *Carbon*. **2015**, *81*, 388-395. doi.org/10.1016/j.carbon.2014.09.071

30. Li, J.-Y.; Liu, Y.; Shu, Q.-W.; Liang, J.-M.; Zhang, F.; Chen, X.-P.; Deng, X.-Y.; Swihart, M. T.; Tan, K.-J. *Langmuir*. **2017**, *33*, 1043-1050. doi:10.1021/acs.langmuir.6b04225

31. Liu, Y.; Zhou, Q.; Yuan, Y.; Wu, Y. *Carbon*. **2017**, *115*, 550-560. doi:10.1016/j.carbon.2017.01.035

32. Sharma, V.; Saini, A. K.; Mobin, S. M. *J. Mater. Chem. B*. **2016**, *4*, 2466-2476. doi.org/10.1039/C6TB00238B

33. Lu, W.; Qin, X.; Liu, S.; Chang, G.; Zhang, Y.; Luo, Y.; Asiri, A. M.; Al-Youbi, A. O.; Sun, X. *Anal. Chem.* **2012**, *84*, 5351-5357. doi:10.1021/ac3007939

34. Du, F.; Zhang, M.; Li, X; Li, J.; Jiang, X.; Li, Z.; Hua, Y.; Shao, G.; Jin, J.; Shao, Q.; Zhou, M.; Gong, A. *Nanotechnology.* **2014**, *25*, 315702-315711. doi:10.1088/0957-4484/25/31/315702

35. Liu, S.; Tian, J.; Wang, L.; Zhang, Y.; Qin, X.; Luo, Y.; Asiri, A. M.; Al-Youbi, A. O.; Sun, X. *Adv. Mater.* **2012**, *24*, 2037-2041. doi:10.1002/adma.201200164

36. Liu, Y.; Zhaoa, Y.; Zhang, Y. *Sens. Actuators, B*. **2014**, *196*, 647-652. doi:10.1016/j.snb.2014.02.053

37. Qin, X. Y.; Lu, W. B.; Asiri, A. M.; Al-Youbi, A. O.; Sun, X. P. *Catal. Sci. Technol*. **2013**, *3*, 1027-1035. doi:10.1039/c2cy20635h

38. Mota, G. S.; Sartori, C. J.; Ferreira, J.; Miranda, I.; Quilhó, T.; Mori, F. A.; Pereira, H. *Ind. Crops Prod*. **2016**, *90*, 65-75. doi:10.1016/j.indcrop.2016.06.014

39. Hill, S. Hill.; Galan, M. C. *Beilstein J. Org. Chem.* **2017**, *13,* 675-693. doi:10.3762/bjoc.13.67

40. Nima, A. M.; Amritha, P.; Lalan, V.; Subodh, G. *J Mater Sci: Mater Electron*. **2020**, *31*, 21767-21778. doi:10.1007/s10854-020-04689-6

41. Han, X.; Zhong, S.; Pan, W.; Shen, W. *Nanotechnology*. **2015**, *26*, 065402-065411. doi:10.1088/0957-4484/26/6/065402

42. Yu, P.; Wen, X.; Toh, Y.-R.; Tang, J. *J. Phys. Chem. C.* **2012**, *116*, 25552-25557. doi:10.1021/jp307308z

43. Zhang, J.; Wang, H.; Xiao, Tang, Y. J.; Liang, C.; Li, F.; Dong, H.; Xu, W. *Nanoscale Res. Lett*. **2017**, 12:611. doi:10.1186/s11671-017-2369-1

44. Kwon, W.; Do, S.; Kim, J.-H.; Seok Jeong, M.; Rhee, S.-W. *Sci Rep*. **2015**, *5*, 12604-12613. doi:10.1038/srep12604

45. Ding, H.; Li, X.-H.; Chen, X.-B.; Wei, J.-S.; Li, X.-B.; Xiong, H.-M. *J. Appl. Phys*. **2020**, *127*, 231101-231121. doi:10.1063/1.5143819

46. Zhu, S.; Meng, Q.; Wang, L.; Zhang, J.; Song, Y.; Jin, H.; Zhang, K.; Sun, H.; Wang, H.; Yang, B. *Angew. Chem. Int. Ed*. **2013**, *52*, 3953-3957. doi:10.1002/anie.201300519

47. Zhu, C.; Zhai, J.; Dong, S. *Chem. Commun*. **2012**, *48*, 9367-9369. doi:10.1039/c2cc33844k

48. Vedamalai, M.; Periasamy, A. P.; Wang, C.-W.; Tseng, Y.-T.; Ho, L.-C.; Shih, C.-C.; Chang, H.-T. *Nanoscale*. **2014**, *6*, 13119-13125. doi:10.1039/c4nr03213f

49. Hsu, P.-C.; Chen, P.-C.; Ou, C.-M.; Chang, H.-Y.; Chang, H.-T. *J. Mater. Chem. B.* **2013**, *1*, 1774-1781. doi:10.1039/c3tb00545c

50. Jiang, C.; Wu, H.; Song, X.; Ma, X.; Wang, J.; Tan, M. *Talanta*. **2014**, *127*, 68-74. doi:10.1016/j.talanta.2014.01.046

51. Li, W.; Yue, Z.; Wang, C.; Zhang, W.; Liu, G. *RSC Adv.* **2013,** *3*, 20662-20665. doi:10.1039/c3ra43330g